Available online at www.sciencedirect.com
ScienceDirect
Corrosion Science 49 (2007) 2254–2269
CORROSION SCIENCE
www.elsevier.com/locate/corsci

Experimental and theoretical study for corrosion inhibition of mild steel in normal hydrochloric acid solution by some new macrocyclic polyether compounds

M. Lebrini [a], M. Lagrenée [a], H. Vezin [c], M. Traisnel [d], F. Bentiss [b,*]

[a] *Unité de Catalyse et de Chimie du Solide, CNRS UMR 8181, ENSCL, BP 90108, F-59652 Villeneuve d'Ascq Cedex, France*
[b] *Laboratoire de Chimie de Coordination et d'Analytique, Faculté des Sciences, Université Chouaib Doukkali, BP 20, M-24000 El Jadida, Morocco*
[c] *Laboratoire de Chimie Organique et Macromoléculaire, CNRS UMR 8009, USTL Bât C4, F-59655 Villeneuve d'Ascq Cedex, France*
[d] *Laboratoire des Procédés d'Elaboration des Revêtements Fonctionnels, PERF UMR 8008, ENSCL, BP 90108, F-59652 Villeneuve d'Ascq Cedex, France*

Received 21 April 2006; accepted 17 October 2006
Available online 16 January 2007

Abstract

New macrocyclic polyether compounds containing a 1,3,4-thiadiazole moiety have been prepared to study the corrosion inhibitive effect of mild steel in normal hydrochloric acid solutions. The salient features obtained from weight loss and electrochemical impedance spectroscopy (EIS) have been discussed. The results of these investigations have shown enhancement in inhibition efficiencies with the extent of the polyethylene glycol unit that forms a cavity. Data obtained from EIS show a frequency distribution and therefore a modelling element with frequency dispersion behaviour, a constant phase element (CPE) has been used.

* Corresponding author. Tel.: +33 320 337 746; fax: +33 320 436 814.
E-mail address: f.bentiss@pop.ensc-lille.fr (F. Bentiss).

0010-938X/$ - see front matter
doi:10.1016/j.corsci.2006.10.029

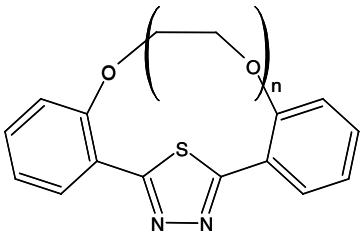

***n*-MCTH** n = 1, 2, 3, 4, 5

Adsorption of *n*-MCTH was found to follow the Langmuir's adsorption isotherm. The thermodynamic functions of adsorption process were calculated from experimental ac impedance data and the interpretation of the results are given. Molecular modelling has been conducted in an attempt to correlate the corrosion inhibition properties with the calculated quantum chemical parameters.

Keywords: Macrocyclic compounds; Corrosion inhibitors; Mild steel; HCl acid; Adsorption process

1. Introduction

The study of corrosion of iron is a matter of tremendous theoretical and practical concern and as such has received a considerable amount of interest [1]. Hydrochloric acid (HCl) solutions are widely used for pickling, cleaning, descaling, etc. of iron and steel. Corrosion inhibitors are needed to reduce the corrosion rates of metallic materials in this acid medium. Different groups of organic compounds have been reported to exert inhibitive effects on the corrosion of mild steel. Compounds containing nitrogen, oxygen and sulphur atoms generally give rise to satisfying inhibitor efficiency in the case of iron corrosion in HCl medium [2–5]. However, data regarding the use of *N*-heterocyclic compounds like thiadiazole derivatives are not so plentiful. In the research on organic corrosion inhibitors, attention is paid to the relationship of inhibitor structure to its inhibition efficiency [6,7], to its adsorption and to the mechanism of adsorption.

Macrocyclic compounds have emerged recently as a new and potential class of corrosion inhibitors. A survey of the literature reveals that despite the high ability of macrocyclic compounds to interact strongly with the metal surface, little attention has been made on use of these compounds as corrosion inhibitors [8–11]. In continuation of our work on the development of thiadiazole derivatives as corrosion inhibitors in acidic media [12–14], we report here the inhibitory behaviour of new macrocyclic polyether compounds (*n*-MCTH) containing a 1,3,4-thiadiazole moiety on corrosion inhibition of mild steel in 1 M HCl solutions. The aim of this work is devoted to study the inhibition characteristics of these compounds for acid corrosion of mild steel using weight loss and electrochemical impedance spectroscopy (EIS). The impedance spectra obtained from this study are analysed to show the equivalent circuit that fits the corrosion data, also the adsorption behaviour of these series are examined. These results are complemented with theoretical calculations in order to provide an explanation of the differences between the probed

inhibitors. Correlation between the inhibition efficiency and the structure of these compounds are presented.

2. Experimental method

2.1. Material preparation

The tested inhibitors; the five macrocyclic derivatives (*n*-MCTH); namely (2,3,8,9-dibenzo-4,7-dioxa-13-thia-11,12-diazabicyclo[8.2.1]trideca-10,12-diene (1-MCTH), 2,3,11,12-dibenzo-4,7,10-trioxa-16-thia-14,15-diazabicyclo[11.2.1]hexadeca-13,15-diene (2-MCTH), 2,3,14,15-dibenzo-4,7,10,13-tretraoxa-19-thia-17,18-diazabicyclo[14.2.1] nona deca-16, 18-diene (3-MCTH), 2,3,17,18-dibenzo-4,7,10,13,16-pentaoxa-22-thia-20,21-diazabicyclo [17.2.1]docosa-19,21-diene (4-MCTH), 2,3,20,21-dibenzo-4,7,10,13,16,19-hexaoxa-25-thia-23,24-diazabicyclo[20.2.1] pentacoza-21,24-diene (5-MCTH), respectively, were synthesised according to a previously described experimental procedure [15]. The molecular formulas of macrocyclic compounds are shown in Fig. 1. Corrosion tests have been carried out on electrodes cut from sheets of mild steel. Steel strips containing 0.09% P, 0.38% Si, 0.01% Al, 0.05% Mn, 0.21% C, 0.05% S and the remainder iron were used for the measurement of weight loss and electrochemical studies. The surface preparation of the specimens was carried out using emery paper nos. 600 and 1200; they were degreased with ethanol under ultrasound and dried at room temperature before use. The solutions (1 M HCl) were prepared by dilution of an analytical reagent grade 37% HCl with doubly distilled water. The solubility of the tested macrocyclic polyether compounds is about 10^{-4} M in 1 M HCl.

2.2. Weight loss method

For weight loss measurements, each run was carried out in a glass vessel containing 100 ml test solution. A clean weighed mild steel electrode ($2 \times 5 \times 0.06$ cm) was completely immersed at inclined position in the vessel. After 24 h of immersion, the electrode was withdrawn, rinsed with doubly distilled water, washed with ethanol, dried and weighed. Duplicate experiments were performed in each case and the mean value of the weight loss has been reported. The weight loss was used to calculate the corrosion rate (W) in milligrams per square centimetre per hour (mg/cm^2 h).

2.3. The electrochemical measurements

Electrochemical impedance spectroscopy measurements were performed using Tacussel Radiometer PGZ 3O1 Frequency Response Analyser in a frequency range of 10^5–10^{-2} Hz with ten points per decade. The electrochemical cell used has been described in previous papers [16,17]. The reference electrode was a saturated calomel electrode. All the reported potential values are referred to this type of electrode. Square sheets of mild steel of size (5 cm by 5 cm by 0.06 cm), which exposed a 7.55 cm^2 surface to the aggressive solution, were used as the working electrode. After the determination of steady-state current at a given potential, sine wave voltages (10 mV) peak to peak were superimposed on the rest potential. Nyquist plots were made from these experiments. The best semicircle can be

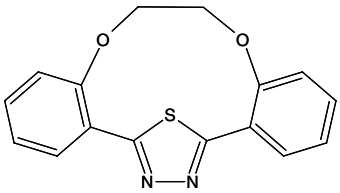

2,3,8,9-Dibenzo-4,7-dioxa-13-thia-11,12-diazabicyclo[8.2.1]trideca-10,12-diene

1-MCTH

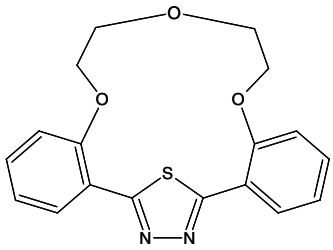

2,3,11,12-Dibenzo-4,7,10-trioxa-16-thia-14,15-diazabicyclo[11.2.1] hexadeca-13,15-diene

2-MCTH

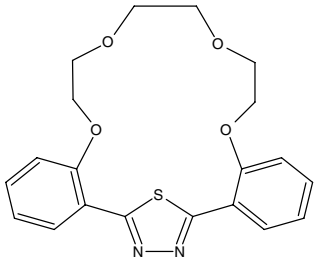

2,3,14,15-Dibenzo-4,7,10,13-tretraoxa-19-thia-17,18-diazabicyclo[14.2.1] nona deca-16,18-diene

3-MCTH

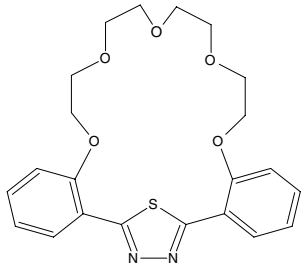

2,3,17,18-Dibenzo-4,7,10,13,16-pentaoxa-22-thia-20,21-diazabicyclo[17.2.1] docosa-19,21-diene

4-MCTH

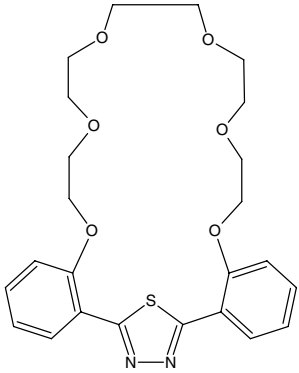

2,3,20,21-Dibenzo-4,7,10,13,16,19-hexaoxa-25-thia-23,24-diazabicyclo[20.2.1] pentacoza-21,24-diene

5-MCTH

Fig. 1. Chemical structures of the investigated macrocyclic derivatives (*n*-MCTH).

fit through the data points in the Nyquist plot using a non-linear least square fit so as to give the intersections with the x-axis [18]. The impedance data were analysed and fitted using graphing and analysing impedance software, version Voltamaster 4.

2.4. Theoretical calculation

The macrocyclic compounds have been fully optimised by using B3LYP Density Functional Theory formalism (DFT) with 6-31G (d, p) basis set with Gaussian 03 code. The following quantum chemical indices were considered: the energy of the highest occupied molecular orbital (E_{HOMO}), the energy of the lowest unoccupied molecular orbital (E_{LUMO}), energy band gap $\Delta E = E_{HOMO} - E_{LUMO}$, the dipole moment ($\mu$), the molecular area and the dihedral angle.

3. Results and discussion

3.1. Weight loss measurements

The corrosion of mild steel in 1 M HCl medium containing various concentrations of n-MCTH ($n = 1, 2, 3, 4, 5$) was studied by weight loss measurements. In this case, E (%) is calculated by applying the following equation:

$$E\% = \left[\frac{W_{corr} - W_{corr(inh)}}{W_{corr}}\right] \times 100 \quad (1)$$

where W_{corr} and $W_{corr(inh)}$ are the corrosion rates of mild steel in the absence and presence of inhibitor molecule, respectively. Table 1 summarizes the corrosion rates (W) of mild steel and the E (%) for the macrocyclic derivatives studied at different concentrations. It is obvious from these data that all of these compounds inhibit the corrosion of mild steel in 1 M HCl solution at all concentrations used in this study and the corrosion rate was seen to decrease with increasing additive concentration at 30 °C. At 1×10^{-4} M, E (%) attains 99.5% for 5-MCTH. Thus, we deduce that this inhibitor is the better inhibitor for the mild steel and E (%) was found to be in the following order: 5-MCTH > 4-MCTH > 3-MCTH > 2-MCTH > 1-MCTH. The difference in their inhibitive action can be explained on the basis of the number of oxygen atoms present in the polyether ring which contribute to the adsorption strength through the donor acceptor bond between the non-bonding electron pairs and the vacant orbitals of the metal surface. As a result of this classification and in order to better understand the inhibition mechanism of n-MCTH, a detailed study using electrochemical impedance spectroscopy was carried out.

3.2. AC impedance studies

Fig. 2 shows Nyquist plots obtained after 24 h of exposure of the mild steel at 30 °C in uninhibited and inhibited solutions containing various concentrations of 1-MCTH. Similar plots are obtained in the case of the other macrocyclic derivatives. It is clear from these plots that the impedance response of mild steel has significantly changed after the addition of n-MCTH in 1 M HCl. The impedance spectra obtained consist of one capacitive loop with one capacitive time constant in the Bode-phase plots (Fig. 3, repre-

Table 1
Corrosion parameters obtained from weight loss of mild steel in 1 M HCl containing various concentrations of *n*-MCTH at 30 °C

Inhibitor	Concentration (M)	W (mg cm^{-2} h^{-1})	E (%)
Blank	–	5.38	–
1-MCTH	1×10^{-6}	2.15	60.0
	1×10^{-5}	0.47	91.2
	5×10^{-5}	0.25	95.2
	1×10^{-4}	0.12	97.7
2-MCTH	1×10^{-6}	1.59	70.3
	1×10^{-5}	0.40	92.5
	5×10^{-5}	0.14	97.4
	1×10^{-4}	0.053	99.0
3-MCTH	1×10^{-6}	1.45	73.0
	1×10^{-5}	0.32	94.0
	5×10^{-5}	0.096	98.2
	1×10^{-4}	0.053	99.0
4-MCTH	1×10^{-6}	1.22	77.2
	1×10^{-5}	0.17	96.7
	5×10^{-5}	0.048	99.1
	1×10^{-4}	0.043	99.2
5-MCTH	1×10^{-6}	1.07	80.0
	1×10^{-5}	0.048	99.1
	5×10^{-5}	0.032	99.4
	1×10^{-4}	0.026	99.5

sentative example). When Nyquist plot contains a "depressed semicircle with the centre under the real axis" (Fig. 4b), such behaviour is characteristic for solid electrodes and often referred to as frequency dispersion which has been attributed to the surface

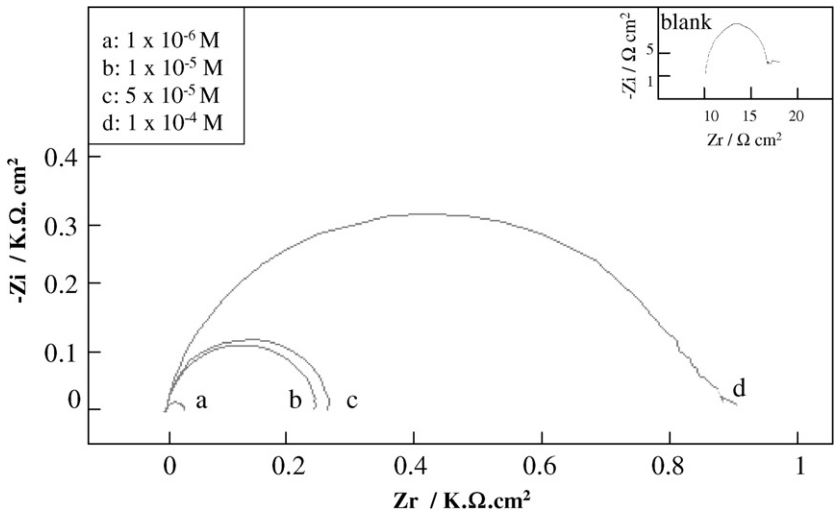

Fig. 2. Nyquist diagrams for mild steel in 1 M HCl containing different concentrations of 1-MCTH at 30 °C.

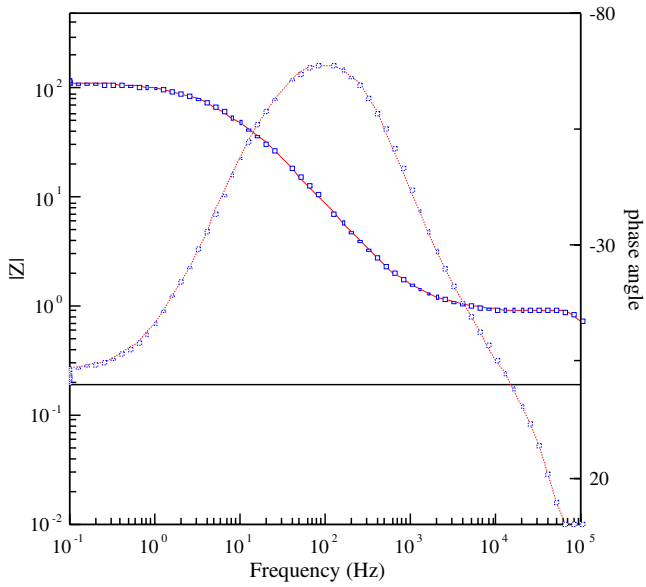

Fig. 3. Bode-phase plots of mild steel in 1 M HCl containing 10^{-4} M of 1-MCTH at 30 °C.

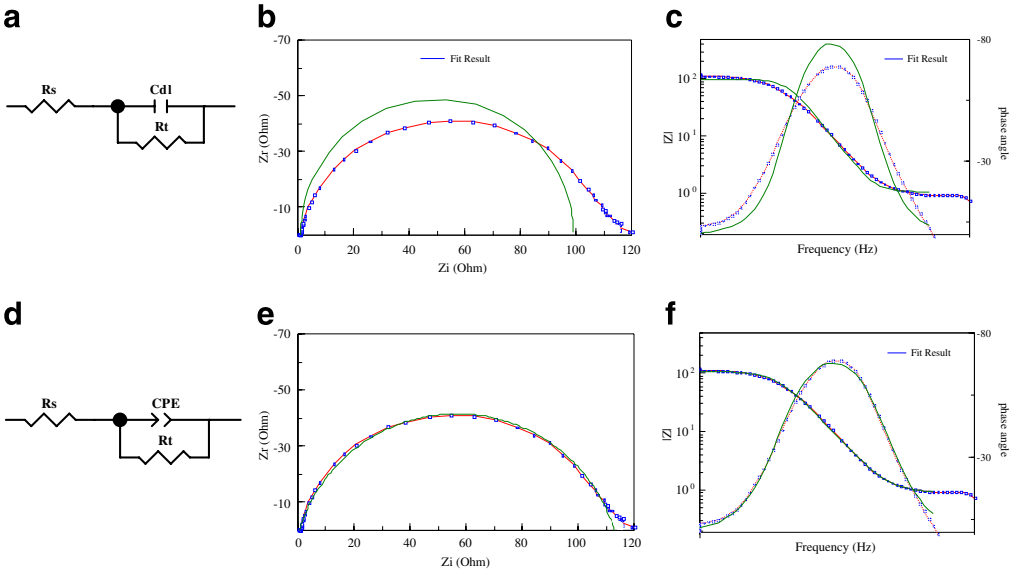

Fig. 4. Equivalent circuit models for mild steel/1 M HCl + 10^{-4} M 1-MCTH interface (a,d) and corresponding impedance diagrams: (b,e) Nyquist plots; (c, f) Bode plots; (···) experimental data; (—) calculated.

heterogeneity due to surface roughness, impurities or dislocations [19–23], fractal structures [19,24,25], distribution of activity centres, inhibitors adsorption and formation of porous layers [23,26,27].

The transfer function can be represented by a resistance R_1 parallel to a capacitor C and in series to them an additional resistance R_2:

$$Z(\omega) = R_1 + \frac{1}{1/R_2 + i\omega C} \tag{2}$$

It can be assumed, on the basis of the statements above, that the transfer function, defined by Eq. (2), is represented by the equivalent circuit shown in Fig. 4a. This transfer function is applicable for homogeneous systems with one time constant when the centre of the semicircle lies on the abscissa.

The classical approach to impedance modelling based on the assumption that the interface model should contain lumped elements only, such as R, C, and L, cannot be applied to this case. This type of modelling suits homogeneous systems in which the space distribution of the parameters is lacking or is insignificant, but an ideal system of this kind is difficult to visualise.

It is evident that it cannot describe the observed depression of the capacitive semicircle and it is necessary to replace the capacitor by some element, which has frequency dispersion like the Constant Phase Element (CPE). This element is a generalised tool, which can reflect exponential distribution of the parameters of the electrochemical reaction related to energetic barrier at charge and mass transfer, as well as impedance behaviour caused by fractal surface structure. On the other hand, there are some cases where the CPE is a formal approximation of the system, having very complicated parameter distribution and it is not possible to give some consistent physical interpretation [19]. The impedance of the CPE is [19,28,29]:

$$Z_{CPE} = A^{-1}(i\omega)^{-n} \tag{3}$$

where A is a proportionality coefficient, ω is the angular frequency (in rad s^{-1}) and $i^2 = -1$ is the imaginary number. n—An exponent related to the phase shift and can be used as a measure of the surface inhomogeneity [19,23]. For whole numbers of $n = 1, 0, -1$ CPE is reduced to the classical lumped elements capacitor (C), resistance (R) and inductance (L). The value of $n = 0.5$ corresponds to Warburg impedance (W). Other values of n approximately describe other types of frequency distribution behaviour of C, R, L or W with distributed parameters.

Fig. 4d shows the electrical equivalent circuit employed to analyse the impedance plots, where the capacitor in Eq. (2) is replaced by a CPE. The resistance R_1 reflects the charge transfer resistance R_t, CPE has the meaning of a frequency distributed double-layer capacitance and R_2 is the resistance of the solution R_Ω. Excellent fit with this model was obtained for all experimental data. As an example, the Nyquist and Bode plots for 1-MCTH are presented in Fig. 4e and f, respectively. The fitted parameters results for n-MCTH, using Zview program, are presented in Table 2. It is observed that this model describes very well these experimental results.

It is obvious from Table 2, that the value of the charge-transfer resistance, R_t increases with the concentration of macrocyclic derivatives. The value of the parameter A of the Z_{CPE} varies in a regular manner with concentration. Its recalculation in terms of capacitor, i.e. in $F\,cm^{-2}$, could serve as a basis of comparison, although roughly. The capacitances were calculated from A and R, using the equation [30–32]:

$$C = (A \cdot R^{1-n})^{1/n} \tag{4}$$

Table 2
Impedance parameters for the corrosion of mild steel in 1 M HCl containing different concentrations of *n*-MCTH and inhibition efficiency values obtained from ac impedance and weight loss studies

Inhibitor	Conc. (M)	$E_{\text{rest potential}}$ vs SCE (mV)	R_t ($\Omega\,cm^2$)	A ($s^n\,\Omega^{-1}\,cm^{-2}\times10^{-3}$)	C ($\mu F\,cm^{-2}$)	n	E (%)	E_{wL} (%)
Blank	0	−510	11.00	2.74	1862.82	0.82	–	–
1-MCTH	1×10^{-6}	−494	29.47	0.73	528.17	0.87	62.7	60.0
	1×10^{-5}	−489	162.8	0.21	120.64	0.86	93.2	91.2
	5×10^{-5}	−490	255.19	0.18	143.01	0.93	95.7	95.2
	1×10^{-4}	−488	813.89	0.06	37.48	0.92	98.6	97.7
2-MCTH	1×10^{-6}	−488	39.22	0.62	424.27	0.87	71.9	70.3
	1×10^{-5}	−490	179.62	0.16	117.58	0.85	93.9	92.5
	5×10^{-5}	−491	400.23	0.068	48.17	0.91	97.2	97.4
	1×10^{-4}	−495	1039.64	0.051	26.61	0.91	98.9	99.0
3-MCTH	1×10^{-6}	−480	47.44	0.557	381.69	0.84	76.8	73.0
	1×10^{-5}	−478	239.11	0.153	109.67	0.91	95.3	94.0
	5×10^{-5}	−485	735.22	0.05	30.70	0.91	98.5	98.2
	1×10^{-4}	−491	1141.56	0.042	22.83	0.90	99.0	99.0
4-MCTH	1×10^{-6}	−487	52.13	0.225	86.47	0.82	78.9	77.2
	1×10^{-5}	−489	545.41	0.079	40.33	0.83	98.0	96.7
	5×10^{-5}	−492	1023.78	0.058	42.98	0.83	98.9	99.1
	1×10^{-4}	−491	1328.80	0.0457	25.72	0.90	99.2	99.2
5-MCTH	1×10^{-6}	−488	62.355	0.140	86.72	0.84	82.3	80.0
	1×10^{-5}	−478	1211.77	0.044	23.59	0.83	99.1	99.1
	5×10^{-5}	−487	1379.38	0.032	20.31	0.87	99.2	99.4
	1×10^{-4}	−490	1554.54	0.031	17.13	0.91	99.3	99.5

A tendency can be seen for decreasing of the capacitance with the concentration of *n*-MCTH. The double-layer between the charged metal surface and the solution is considered as an electrical capacitor. The decrease of C with increasing macrocyclic derivatives concentrations may be attributed to the formation of a protective layer at the electrode surface.

The increase of the values of n when compared with 1 M HCl and with concentration can be explained by some decrease of the surface heterogeneity, due to the adsorption of the inhibitor on the most active adsorption sites [20]. In the case of impedance study, E (%) is calculated by R_t as described elsewhere [17]. The efficiency values are given in Table 2. E (%) of macrocyclic derivatives tested decreases in the order 5-MCTH > 4-MCTH > 3-MCTH > 2-MCTH > 1-MCTH. The inhibition efficiencies, calculated from ac impedance study, show the same trend as those obtained from weight loss measurements. Comparison of the E (%) values obtained using these methods show acceptable agreement (Table 2). The comparative study of the macrocyclic derivatives by weight loss measurements and ac impedance study indicated that E (%) was dependent on the number of oxygen atoms present in the polyether ring.

3.3. Adsorption isotherm

Adsorption isotherms are very important in understanding the mechanism of organo electrochemical reactions [33]. In order to obtain the isotherm, the fractional coverage values θ, as a function of inhibitor concentration, must be obtained. θ can be obtained from the impedance measurements as described elsewhere [33]. It is preferable to evaluate the adsorption isotherm with ac impedance study because the imposed sine wave voltages, at 10 mV peak to peak, does not disturb the surface, therefore no desorption occurs in this case. The best correlation between the experimental results and isotherm functions was obtained using Langmuir adsorption isotherm. The Langmuir isotherm for monolayer chemisorption is given by the following equation [34]:

$$\frac{C_{inh}}{\theta} = \frac{1}{K} + C_{inh} \tag{5}$$

where θ is the surface coverage degree, C_{inh} is the inhibitor concentration in the electrolyte and K the equilibrium constant of the adsorption process. The plot of C_{inh}/θ versus C_{inh} of 1-MCTH yields a straight line with correlation coefficient more than 0.99 showing that the adsorption of this inhibitor can be fitted to Langmuir adsorption (Fig. 5). Similar behaviour is observed in the case of the other macrocyclic derivatives. It is found that all the values of the slopes are very close to 1. These isotherms conform to Langmuir type, suggesting monolayer chemisorption of the *n*-MCTH. From the intercepts of the straight lines C_{inh}/θ-axis, K values were calculated and are given in Table 4. The constant of adsorption, K, is related to the standard free energy of adsorption, ΔG^0_{ads}, with the following equation [35]:

$$K = \frac{1}{55.5} \exp\left(\frac{-\Delta G^0_{ads}}{RT}\right) \tag{6}$$

where R is the universal gas constant and T is the absolute temperature. The standard free energy of adsorption (ΔG^0_{ads}) can be calculated (Table 3). ΔG^0_{ads} is expressed in kJ mol^{-1} of Org_{ads}. The negative values of ΔG^0_{ads} ensure the spontaneity of the adsorption process and

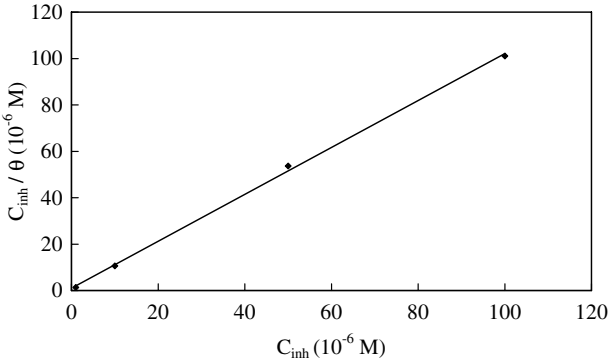

Fig. 5. Langmuir adsorption plot for mild steel in 1 M HCl containing different concentrations of 1-MCTH at 30 °C.

Table 3
The values of K and ΔG^0_{ads} of macrocyclic derivatives for mild steel in 1 M HCl at 30 °C

Inhibitor	K (10^6 M^{-1})	ΔG^0_{ads} (kJ mol^{-1})
1-MCHT	1.018	−44.94
2-MCHT	2.052	−46.71
3-MCHT	2.605	−47.31
4-MCHT	7.032	−49.81
5-MCHT	19.342	−52.36

stability of the adsorbed layer on the steel surface. Generally, values of ΔG^0_{ads} around -20 kJ mol^{-1} or lower are consistent with the electrostatic interaction between the charged molecules and the charged metal (physisorption); those around -40 kJ mol^{-1} or higher involve charge sharing or transfer from organic molecules to the metal surface to form a coordinate type of bond (chemisorption) [36,37]. The calculated ΔG^0_{ads} values of slightly more negative than -40 kJ mol^{-1} indicate, therefore, that the adsorption mechanism of the macrocyclic derivatives on steel in 1 M HCl solution is typical of chemisorption (Table 3). The large negative value of ΔG^0_{ads} in the case of 5-MCTH indicate that this inhibitor is strongly adsorbed on the steel surface [38]. Moreover, $|\Delta G^0_{ads}|$ of n-MCTH decreases in the order 5-MCTH > 4-MCTH > 3-MCTH > 2-MCTH > 1-MCTH. This is in good agreement with the values of inhibition efficiency obtained from the weight loss and electrochemical techniques.

3.4. Quantum chemical study

Quantum structure–activity relationships (QSAR) have been used to study the effect of molecular structure on inhibition efficiency of macrocyclic compounds (n-MCTH). We have performed molecular modelling in order to understand if any structural differences induced by the number of oxygen atoms present in the polyether ring can be reliable to the observed differences of the corrosion inhibition efficiency. In this way, the macrocyclic compounds have been fully optimised using density functional theory method (DFT). The major structural differences between the molecules are due to the dihedral angle modifications between

Table 4
Calculated quantum chemical indices of macrocyclic polyether derivatives

Compound	E_{HOMO} (eV)	E_{LUMO} (eV)	ΔE (eV)	μ (Debye)	Molecular area (Å^2)	Dihedral angle C–C–C–S (Degree)
1-MCTH	−6.04	−1.57	−4.47	5.37	301.85	−10.28
2-MCTH	−5.60	−1.36	−4.24	6.51	346.57	−2.87
3-MCTH	−5.61	−1.52	−4.09	4.89	395.88	3.67
4-MCTH	−5.55	−1.44	−4.11	6.70	459.54	9.05
5-MCTH	−5.66	−1.52	−4.14	5.04	515.27	19.665

the aromatic cycles and the thiadiazole frame (C–C–C–S). The values of these dihedral angles and the other calculated quantum chemical indices of *n*-MCTH are reported in Table 4. The structures and electrostatic potential maps for *n*-MCTH are depicted in Figs. 6–10. The quantum parameters are closed together. Effectively, the variation of the calculated HOMO and LUMO energies are in the magnitude of 0.5 eV energy differences between all the macrocyclic derivatives.

In this way, a linear equation was used to correlate all quantum chemical parameters (E_{LUMO}, E_{LUMO}, μ) and inhibitor concentration (C_{inh}) with experimental inhibition efficiencies. The linear model proposed by Bentiss et al. [39] for the interaction of corrosion

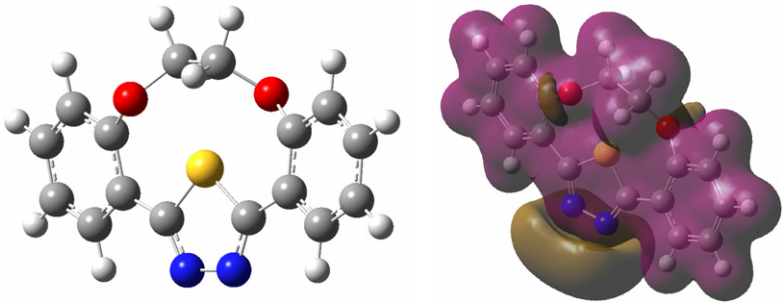

Fig. 6. Structure and electrostatic potential map for 1-MCTH.

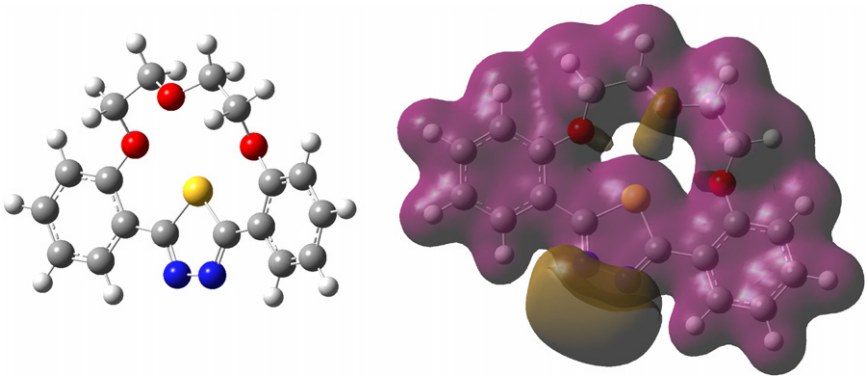

Fig. 7. Structure and electrostatic potential map for 2-MCTH.

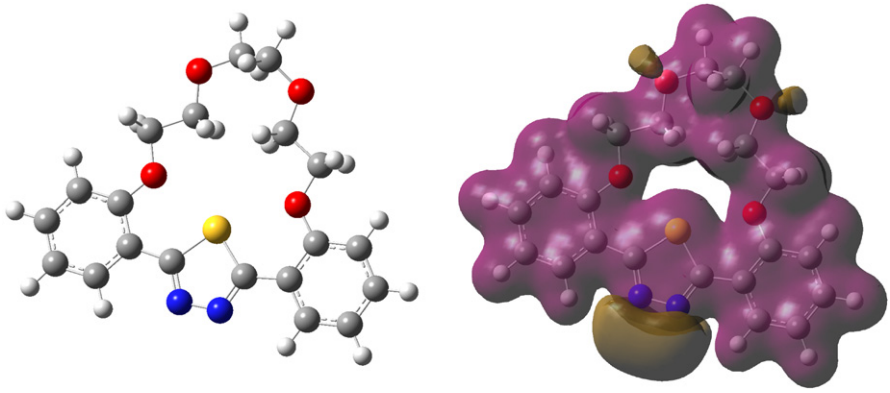

Fig. 8. Structure and electrostatic potential map for 3-MCTH.

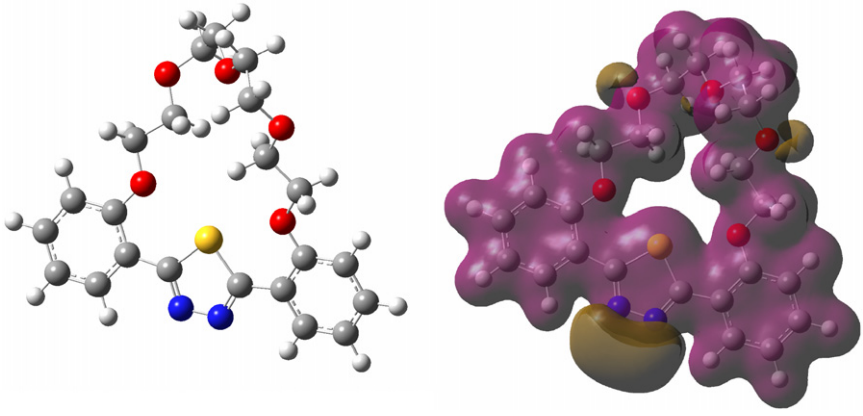

Fig. 9. Structure and electrostatic potential map for 4-MCTH.

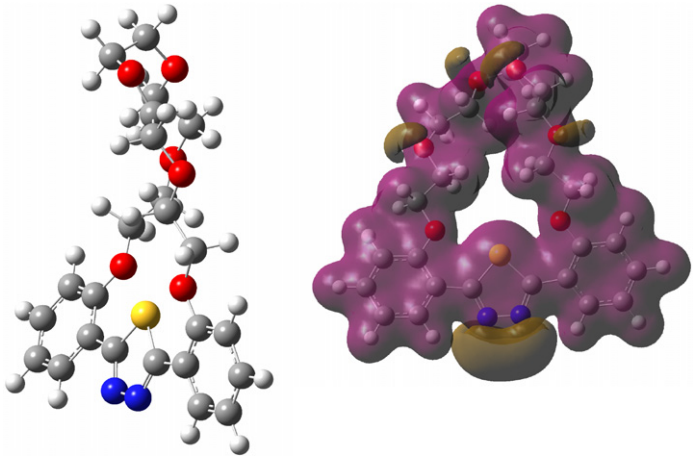

Fig. 10. Structure and electrostatic potential map for 5-MCTH.

inhibitors with metal surface in acidic solutions has been used in this study. The general equation describing the QSAR linear model used can be expressed as follows:

$$Rt_i = \sum_j (A\mu_j + BE_{\mathrm{HOMO}j} + CE_{\mathrm{LUMO}j})C_{\mathrm{inh}i}(\mathrm{LR}) \tag{7}$$

where R_t is the charge transfer resistance, A, B, and C are the regression coefficients of the calculated quantum chemical parameters for the molecule j and $C_{\mathrm{inh}i}$ denotes the concentration of the inhibitor in experiment i.

Experimental and calculated values of R_t are displayed in Fig. 11. The best regression equation for *n*-MCTH, obtained by using the LR model was:

$$R_t = 5 + (2.710^7 E_{\mathrm{HOMO}} - 7.610^7 E_{\mathrm{LUMO}} + 3.910^6 \mu)C_{\mathrm{inh}} \quad N = 20,$$
$$R = 0.90, \quad F_{\mathrm{obs}} = 23, \quad F_{(0,99)} = 7.59 \tag{8}$$

where R denotes the correlation coefficient and N is the total number of experimental impedances. The significance of the regression equation was obtained by calculating the Fischer's F number [40]. The coefficient of E_{LUMO} in Eq. (8) is negative. This fact proves that d-orbitals of steel accept electrons from the macrocyclic compounds and feed back bonds form between steel and inhibitor molecules. Forming of feed back bond increases chemical adsorption of *n*-MCTH molecules on the steel surface and so increases the inhibition efficiencies of these compounds. A highly significant correlation coefficient ($R = 0.90$) between experimental and estimated values of R_t was obtained (Fig. 11). This significant correlation indicated that the variation of the corrosion inhibition with the structure of the inhibitors may be explained in terms of electronic properties. In our present case, the corrosion inhibition efficiency can be explained not only in terms of electron orbital analysis but also seems to depend on the geometry of these molecules. The difference in their inhibitive action can be explained on the basis of the number of oxygen atoms present in the polyether ring which contribute to the chemisorption strength through the donor acceptor bond between the non-bonding electron pair and the vacant orbitals of the metal

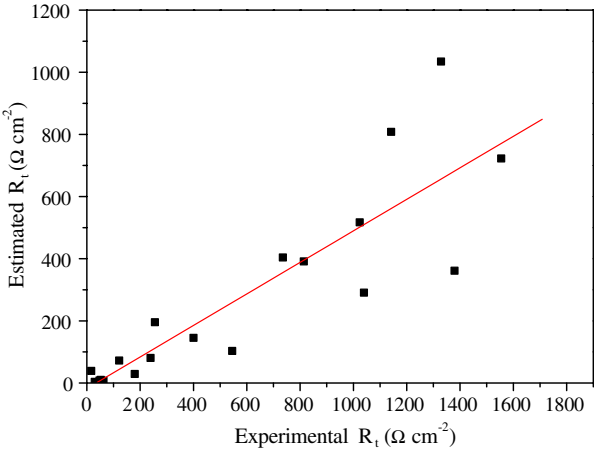

Fig. 11. Experimental and predicted R_t values of *n*-MCTH by the LR model.

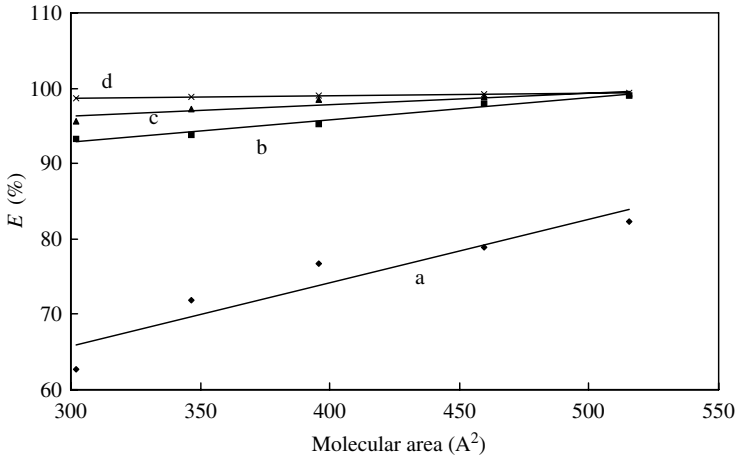

Fig. 12. Correlation of the molecular area and the inhibition efficiency values of *n*-MCTH from ac impedance method, at different concentrations: (a) 10^{-6} M, (b) 10^{-5} M, (c) 5×10^{-5} M, (d) 10^{-4} M.

surface. The calculated electrostatic potential maps reveal a good distribution of the negative charge along the molecule for the *n*-MCTH. The electrostatic potential is principally distributed on nitrogens and some oxygen atoms with respect to the structure (Figs. 6–10). Moreover, the molecular area increases with the number of oxygen atoms present in the polyether ring and hence this parameter play an important role when comparing the inhibition properties of these macrocyclic compounds (Table 4). The correlation between the molecular area values and the inhibition efficiency values from ac impedance method, at different concentrations, is shown in Fig. 12. The values of the correlation of the linear relationship are 0.89–0.98. It can be seen that E (%) increases with the increase of the values of the molecular area, favouring their adsorption ability.

4. Conclusions

Macrocyclic compounds (*n*-MCTH) are effective inhibitors of corrosion of mild steel exposed to 1 M HCl solution. Their inhibition efficiencies increase with inhibitors concentration in the order of 5-MCTH > 4-MCTH > 3-MCTH > 2-MCTH > 1-MCTH and attain the maximum value of 99.5% at 10^{-4} M of 5-MCTH. The weight loss and ac impedance are in reasonably good agreement. The Langmuir adsorption isotherm provides a formal description of the adsorptive behaviour of *n*-MCTH on mild steel. The ΔG^0_{ads} values reveal that the corrosion inhibition by *n*-MCTH is due to the formation of a chemisorbed film on the metal surface. The difference in their inhibitive action can be explained on the basis of the number of oxygen atoms present in the polyether ring which contribute to the chemisorption strength through the donor acceptor bond between the non-bonding electron pair and the vacant orbital of the metal surface. Using QSAR approach we have established a direct correlation, for *n*-MCTH, between their molecular structure and their E (%) by using a linear resistance (LR) model joining the R_t to chemical quantum parameters. A highly significant multiple correlation coefficient ($R \sim 0.90$) has been obtained between experimental and predicted R_t using the LR model.

References

[1] S.A. Ali, M.T. Saeed, S.V. Rahman, Corros. Sci. 45 (2003) 253.
[2] K.C. Pillai, R. Narayan, Corros. Sci. 2 (1983) 3.
[3] J.O'M. Bockris, J. McBreen, L. Nanis, J. Electrochem. Soc. 112 (1965) 1025.
[4] F. Bentiss, M. Traisnel, H. Vezin, H.F. Hildebrand, M. Lagrenée, Corros. Sci. 46 (2004) 2781.
[5] M. Lagrenée, B. Mernari, M. Bouanis, M. Traisnel, F. Bentiss, Corros. Sci. 44 (2002) 573.
[6] W. Durnie, R. De Marco, A. Gefferson, B. Kinsella, J. Electrochem. Soc. 146 (1999) 1751.
[7] V.S. Sastri, J.R. Perumareddi, Corrosion 53 (1997) 617.
[8] S. Hettiarachi, Y.W. Chan, R.B. Wilson, V.S. Agarwala, Corrosion 45 (1989) 30.
[9] F.R. Longo, J.J. Dellucia, V.S. Agarwala, Proc. 6th European Symposium on Corrosion Inhibitors, Univ. Ferrara, Italy, 1985, p. 155.
[10] V.S. Agarwala, Proc. Int. Cong. Metallic Corros. 1 (1984) 380.
[11] V.N.S. Pillai, J. Thomas, P.S. Harikumar, Indian J. Chem. Technol. 2 (1995) 93.
[12] F. Bentiss, M. Traisnel, M. Lagrenée, J. Appl. Electrochem. 31 (2001) 41.
[13] M. El Azhar, B. Mernari, M. Traisnel, F. Bentiss, M. Lagrenée, Corros. Sci. 43 (2001) 2229.
[14] F. Bentiss, M. Lebrini, H. Vezin, M. Lagrenée, Mater. Chem. Phys. 87 (2004) 18.
[15] F. Bentiss, M. Lebrini, M. Lagrenée, J. Heterocyclic Chem. 41 (2004) 419.
[16] F. Bentiss, M. Lagrenée, M. Traisnel, J.C. Hornez, Corros. Sci. 41 (1999) 789.
[17] F. Bentiss, M. Lagrenée, M. Traisnel, J.C. Hornez, Corrosion 55 (1999) 968.
[18] E. McCafferty, V. Pravdic, A.C. Zettlemoyer, T. Faraday Soc. 66 (1999) 237.
[19] Z.B. Stoynov, B.M. Grafov, B. Savova-Stoynova, V.V. Elkin, Electrochemical Impedance, Nauka, Moscow, 1991.
[20] F.B. Growcock, R.J. Jasinski, J. Electrochem. Soc. 136 (1989) 2310.
[21] G. Reinhard, U. Rammelt, Proc. 6th European Symposium on Corrosion Inhibitors, Univ. Ferrara, 1985, p. 831.
[22] P. Li, J.Y. Lin, K.L. Tan, J.Y. Lee, Electrochim. Acta. 42 (1997) 605.
[23] D.A. Lopez, S.N. Simison, S.R. de Sanchez, Electrochim. Acta. 48 (2003) 845.
[24] W.H. Mulder, J.H. Sluyters, Electrochim. Acta. 33 (1988) 303.
[25] A.H. Mehaute, G. Grepy, Solid State Ionics 910 (1983) 17.
[26] A.A. Hermas, M.S. Morad, M.H. Wahdan, J. Appl. Electrochem. 34 (2004) 95.
[27] A. Popova, S. Raicheva, E. Sokolova, M. Christov, Langmuir 12 (1996) 1083.
[28] Z. Stoynov, Electrochim. Acta. 35 (1990) 1493.
[29] J.R. Macdonald, J. Electroanal. Chem. 223 (1987) 25.
[30] S. Martinez, M. Metikos-Hukovic, J. Appl. Electrochem. 33 (2003) 1137.
[31] X. Wu, H. Ma, S. Chen, Z. Xu, A. Sui, J. Electrochem. Soc. 146 (1999) 1847.
[32] H. Ma, X. Cheng, G. Li, S. Chen, Z. Quan, S. Zhao, L. Niu, Corros. Sci. 42 (2000) 1669.
[33] N. Hackerman, E. McCafferty, in: Proc. 5th International Congress on Metallic Corrosion, vol. 4, 1974, p. 542.
[34] R. Agrawal, T.K.G. Namboodhiri, Corros. Sci. 30 (1990) 37.
[35] J. Flis, T. Zakroczymski, J. Electrochem. Soc. 143 (1996) 2458.
[36] F.M. Donahue, K. Nobe, J. Electrochem. Soc. 112 (1965) 886.
[37] E. Kamis, F. Bellucci, R.M. Latanision, E.S.H. El-Ashry, Corrosion 47 (1991) 677.
[38] J.D. Talati, D.K. Gandhi, Corros. Sci. 23 (1983) 1315.
[39] F. Bentiss, M. Traisnel, H. Vezin, M. Lagrenée, Corros. Sci. 45 (2003) 371.
[40] G.W. Snedecor, W.G. Cochran, Statistical Methods, Iowa State University Press, Ames, IA, 1972, p. 117.